The Nucleus ***52****, No. 4 (2015) 159-164*

www.thenucleuspak.org.pk

The Nucleus

ISSN 0029-5698 (Print)

ISSN 2306-6539 (Online)

Molecular Imaging of CaO Nanowhiskers in Living Organs

A.R. Butt[1*], I.A. Butt[2], A. Nazir[3], M. Ikram[4], S. Sadiq[5], K. Rashid[1,6], T. Shujah[1] and S. Ali[1,7]

[1]*Material and Nano Science Research Lab (MNRL), Department of Physics, Government College University, Lahore, Pakistan*

[2]*Mayo Hospital, Lahore, Pakistan*

[3]*Department of Physics, International Islamic University, Islamabad, Pakistan*

[4]*Solar Applications Research Lab, Department of Physics, Government College University, Lahore, Pakistan*

[5]*Avicenna Medical College, Lahore, Pakistan*

[6]*Applied Physics & Computer Center, Pakistan Council for Scientific and Industrial Research, Lahore, Pakistan*

[7]*Department of Physics, Government College University, Lahore, Pakistan*

aibutt2009@gmail.com; iftikharbutt88@yahoo.com; asma.phdphy5@iiu.edu.pk; mianraj.1981@gmail.com; sobia259@yahoo.com; khalid_pcsir@yahoo.com; tahira_gcu@hotmail.com; salamat601@yahoo.com

ARTICLE INFO

Article history :

Received : 17 August, 2015

Revised : 10 November, 2015

Accepted : 12 December, 2015

Keywords :

Calcium Oxide
Molecular Imaging
Toxicity
Antimicrobial
Bio labeling

ABSTRACT

Nanomaterials are potential ingredients in the diagnostics and drug delivery of various neurological disorders. Calcium oxide (CaO) nanowhiskers were utilized in rats for molecular imaging in liver, kidney and brain. X-ray diffraction (XRD) describes a cubic phase crystal structure of CaO ranges between ~ 4 - 11 nm. Thermo-gravimetric analysis (TGA) shows that these nanostructures are stable above 953K. Scanning Electron microscope (SEM) image depicts the agglomerated nanowhiskers formation while Energy Dispersive X-ray (EDX) also confirms the only presence of Ca and O. These nanostructures were enwrapped with polyvinyl alcohol (PVA) as a biological marker. Necrosis, hemorrhages and degenerations were seen histopathologically in kidney, liver and brain following three months of administration of CaO nanostructures in the degree of severity. Immunofluorescence contemplate likewise could not distinguish any neuro-inflammations.

1. Introduction

Optical imaging is a sophisticated technique for diagnostic tumor imaging. This is a sensitive and non-destructive method. Optical imaging system comprises of two major components i.e. imaging component and optical contrast enhancing component. Imaging component has being upgraded by utilizing laser as a light source coupled with Charged Coupled Device (CCD) and improved by rigorous mathematical modeling of its propagation in biological tissues. UV sources are limited for ex-vivo optical contrast image because its deep penetration is not possible through tissues. However, Near Infra-Red Rays (NIR)are highly advantageous as they can be easily absorbed to a larger depth of about a few cm, in this way by improving sensitivity give more anatomical insights about tissues and skull [1].

Nanomaterials are the most promising materials to be utilized in electrical, optical and magnetic applications [2]. Nano-biomedical applications need these peculiarities to be modulated [3-8]. The efficacies of the nano-therapeutics drugs have been enhanced by reducing their toxicity level, so that they can be potentially utilized in for cell separation & purification and overcoming biological barriers as targeted drug delivery agents [9-11] .

Despite of the advancements and discoveries in therapeutic drugs, the hindrances in the medications of neurological disorder are still limited because of their inefficient delivery to Central Nervous System (CNS) [12]. Globally, the development rate of CNS nanodrugs should be over 500% comparable to cardiovascular drugs [13]. Blood brain barrier breaching can be possible by those drugs with sub-atomic mass (< 400 – 500 Da) and high lipid solubility [14].

The functionalization of nanoparticles (NPs) is necessary to modulate certain characteristics like increasing drug transport capability, binding to targeted organ and their ultimate defecations [15]. Subsequently, the kinetics and efficiency of drugs can be improved through different tissues making an effective transport mechanism [15]. After such improvements in NPs, fluorescent dyes are used as biomarkers for in-vivo ocular imaging [15].

* Corresponding author

Inorganic nanoparticles have been turning out to be more significant for a decade because of their distinctive size dependent physicochemical and material properties. Their biological features, stability, inertness and surface functionality mark them a captivating replacement of organic based nanoparticles for theranostics purposes. But the chronic effects i.e. inflammation, tissue damage, immunogenicity, toxicity and carcinogenicity produced by these nanoparticles are not obvious and still require a series of investigations prior to clinical trial [16]. Therefore, it is important to architect such inorganic nanoparticles that cannot possibly minimize these inadmissible effects while optimizing the necessities of short-term therapeutics [16]. In literature, a lot of experiments are reported investigating the antimicrobial behavior of nanomaterials [17]. Recently, inorganic metallic oxides have shown more potential to influence microorganism in diverse areas, most specifically in dentistry. Anti-microbial activity depends on the particle size of the metallic oxides which is dependent on their morphologies [18]. Hence, synthesis and processing techniques are mandatory to make nanostructures with varied size distributions and morphological configurations [19-21].

It is also reported that various metallic nano-oxides such as CaO, ZnO and MgO are thermally stable with high antimicrobial action [22]. Because of antimicrobial and histo-compatibility [23, 24], CaO is widely considered in tissue dissolution [25], and to deactivate microbial endotoxin [26, 27]. Pure cubic crystalline nature of CaO exhibits anisotropic catalytic behavior and used as dopant to stabilize metal-oxide. A small number of research groups described the synthesis of nanosized CaO employing two methods i.e. sol-gel and thermal decomposition [22].

In this research, co-precipitation was opted to synthesis CaO nanostructures. Their crystallite size and morphology was observed by XRD and SEM. Their thermal degradation was monitored through DSC/TGA and then was applied on different rat organs (liver, kidney and brain). Confocal microscopy was carried out to access neuro-inflammation in the body while antibody conjugated nanoparticle was assessed by immunofluorescence.

2. Experimental details

2.1 Materials

Calcium chloride ($CaCl_2$), sodium hydroxide (NaOH), polyvinyl alcohol (PVA) and ethanol were bought from Sigma Aldrich. For immune-histochemistry (IMC), MetOH, Trizma non saline (TNS), 0.2% Triton X-100 in Trizma base solution (TXTBS), Trizma base solution (TBS), Phosphate buffer saline (PBS) 1X, 4% para formaldehyde, primary antibody, secondary antibodies 3% Normal Horse Serum (NHS, S-2000), distilled water and cryoprotective media were prepared and utilized [28]. Goat anti-mouse Cy3 was obtained from Jackson Immuno Research, Euthatal, xylene and DPX Mounting media (1330-20-7) were received from Merck.

2.2 Synthesis of CaO Nanowhiskers

Co-precipitation technique was used for the synthesis of CaO nanowhiskers [29-31]. In this method, the aqueous solutions of sodium hydroxide (NaOH) and calcium chloride ($CaCl_2$) were separately prepared in distilled water. An aqueous solution of $CaCl_2$ was dripped slowly in an aqueous solution of NaOH while vigorously stirring (80 °C, 60 min) to obtain white supersaturated suspension of calcium hydroxide ($Ca(OH)_2$). This suspension was washed several times in hydro-alcoholic liquids to flush NaCl and other byproducts produced during reaction, thereby enhancing its stability by reducing agglomeration [32]. The resulting suspension was let to permeate through syringe filter and dried (60°C for 24 hours). The obtained nanopowder was heated in furnace (450°C) and kept in a desiccator for storage. CaO nanomaterial was loaded with polyvinyl alcohol (PVA) under constant thermal stirring at 55 ºC [31, 33]. Finally, loaded CaO nanomaterial was used in rats for in-vivo and ex-vivo analysis.

2.3 Characterization

The structural characterization was carried out by XRD diffractometer (PANalytical XPert PRO, $\lambda = 1.5406$ Å). The thermal transitions within CaO were inspected by thermogravimetric / differential scanning calorimetric (TGA-DSC) on SDT Q600 (TA instrument). The morphology and compositional analysis were observed by JEOL 648OLV scanning electron microscope (SEM) and Energy dispersive Spectrometer (EDS), respectively.

2.4 Toxicity Examination

All studies were conducted in accordance with UK animal's scientific procedures act 1986 and the University of Cambridge ethical review panel. We took 5 weeks old SHR (Spontaneous hypertensive) rats from the Cambridge University animal facility and individually housed in cages. They were provided with commercial feed, ad-libitum and drinking water under standard temperature. Each rat was SC injected with 150 µl of PVA coated CaO in PBS buffer rat [31, 33] and observed week by week for any clinical indications of toxicity. After 3 months, the experiment was ended and the rats were sacrificed by intra-peritoneal injection (30mg/100g, sodium pentobarbitone). The brain sections were perfused and were quickly removed to store for overnight (4°C, in 4% of paraformaldehyde). Brain tissues and were placed for cryo-protectionin 30% sucrose [28].

2.4.1 Histopathology

The tissue specimens were collected from all living organs i.e. skin, muscle, brain, kidney & liver. After perfusion and fixation, these specimens were processed in different ethanol dilutions and hematoxylin and eosin (H&E) staining agents for histo-investigations.

2.5 Bio-conjugation of Nanowhiskers

Five male SHRs (~5 weeks old) were chosen. The procedure was intended to use the least number of rats which were sufficient to acquire important results. For this purpose middle-cerebral artery (MCA) occlusion model described by Buchan et al was adopted [31, 34-36]. After occlusion of 15 min, the rats were set free for about 3 months and then the experiment was terminated by following perfusion-fixative of brain cells for immune-fluorescence assay.

2.5.1 Cryo-sectioning

Brain sections were rapidly separated from the skull and post-fixed in 4% PFA solution at 4°C overnight and submerged in 0.1 M PBS with sucrose 30% (3-4 days). The harvested brain from each rat was put onto a sample shuttle of sledge microtome and cut for coronal segment series (40μm). Different sections were taken from the minor/ interior forceps of corpus callosum to the superior colliculi (Bregma 3.7 to 6.80 mm) and the visual cortex and fixed on gelatin-glazed slides [28, 31].

2.5.2 Immunofluorescence for localization of CaO nanostructures

For immune-fluorescence assay, brain cryosections were quenched with CH_3OH and H_2O_2 (10%, 5min) and kept in a solution containing 3% NHS in TXTBS (2 hours). 2 ml solution of nanowhiskers was prepared in PBS for specific bindings with different primary antibodies. Sections were overnight incubated at 4 °C in this solution. After then, sections were washed with TBS and incubated in TXTBS containing secondary antibody anti-mouse Cy3 (1: 150, Jackson Immuno Research, 2 hours). After washing, the sections were mounted on gelatine-coated slides, dried for 15 minutes on a heating block (40 °C) and slip-coverd using FluorSave reagent (Calbiochem) [31].

2.6 Microscopic assessment of ischemic lesions

The stained slides were scanned at 200x on Ariol SL 50 (Applied Imaging, Santa Clara, USA) and captured with a microscope (BX61, Olympus) integrated to the system. The composite images were stitched automatically from individual frames.

3. Results and Discussions

XRD pattern of as-prepared CaO nanostructures was analysed with the standard database from International Centre for Diffraction Data (ICDD) to identify the various phases appeared (Fig. 1). Pure cubic phase of CaO was confirmed through ICDD Card No. 00-017-0912; having space group Fm-3m. The peaks also showed the crystalline nature of CaO with mean crystallite size given by Scherrer formula [37].

$$Crystallite\ size = \frac{0.94\lambda}{\beta Cos\theta}$$

Where β is the peak broadening at half maxima at corresponding Bragg's angle. The crystallite size ranges from 4 – 11 nm.

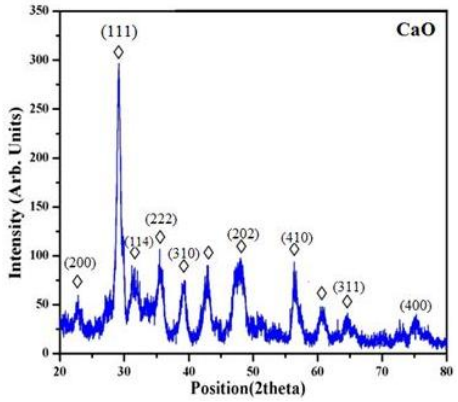

Fig.1: X-ray diffraction pattern of the prepared nanostructures

Thermal degradations were monitored by TGA/DSC from 0°C to 800°C as shown in Fig. 2. DSC curve quantified three prominent endothermic peaks with mass loss at three stages. Firstly, the mass loss (50-200 ºC) was owed to the release of hydroxyl groups within the hydrated nanomaterial. Secondly, mass loss observed (380-420) °C is attributed to the evaporation of organic solvents used in reactions. Thirdly, a drastic mass change appeared (450–550) °C is due to the decomposition of $Ca(OH)_2$ in CaO.

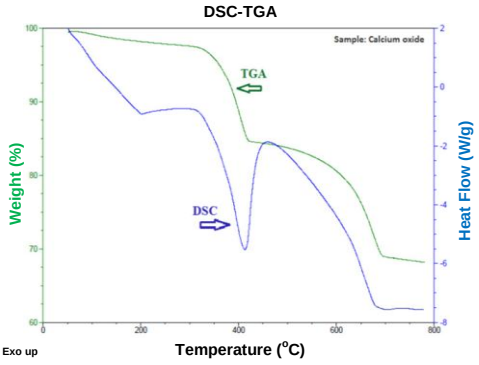

Fig. 2: Thermal analysis of CaO nanowhiskers

No specific structure of nanomaterial could be estimated at 3000 magnification from the SEM image as shown in Fig. 3a whereas, an agglomerated architecture of CaO nanowhiskers is obvious at a further magnification of 10000 times (Fig. 3b).

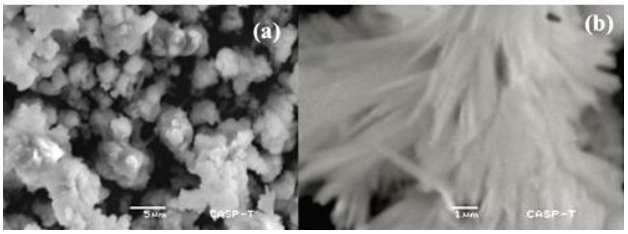

Fig. 3: SEM images of CaO at (a) 3000x and (b) 10,000x

3.1 Histopathological Evaluation

The inflammatory responses of PVA coated CaO nanostructures on different organs are shown in Table 1. Skin tissues revealed no discernible lesions or degenerative changes and all three dermal layers, i.e. epidermis, dermis and hypodermis were fairly intact. It was observed that the architecture of capillary tubes is normal while that of the elastic fibers and collagen are distorted. Likewise, no observable pathological changes were observed in the muscle samples from the majority of the animals and muscle fibers remained intact.

Table 1: Table Caption is missing

Nanomaterial	Skin	Muscle	Liver	Kidney	Brain
PVA-CaO	-	-	+	++	+

-: no remarkable change, + : mild change, ++ : excessive change

The potency of CaO nanowhiskers to damage the tissue was observed by histopathological photos of liver, kidney and brain as shown in Fig. 4 respectively. In Fig. 4a, CaO augmented a number of morphologically distorted and disoriented hepatocytes which was significantly evident all over the hepatic parenchyma, while the higher resolution investigation revealed severely distorted hepatocytes undergoing necrotic changes, which depicted pathological condition of sub-acute severe hepatic degeneration and necrosis.

Fig. 4b shows that severe tubular hemorrhages, renal tubular necrosis and tubular parenchymatous degeneration in kidneys were observed and represented with arrows. Moreover, histological investigations revealed that the renal tubular cells were distended, pyknotic, and were morphologically diagnosed as sub-acute severe renal tubular degeneration and necrosis . Similarly, few incidences of perivascular coughing and mild hemorrhages (arrows) were observed in brain sections of rat (Fig. 4c).

3.2 Immunofluorescence

Immunofluorescence assay was carried out to observe the localization of neuro-inflammation by antibody conjugated CaO nanowhiskers. No neuro-inflammatory localization could be detected (Fig. 5) as antibodies bindings with CaO were missing. This effect may be due to multiple reasons: (i) Perhaps, using NeuN, OX42 and GFAP antibodies with a fluorescent molecule (goat anti-mouse Cy3) can serve as a control (ii) or as CaO has antimicrobial behavior, so it may react against microbes to kill them, that's why no antibodies bindings were observed.

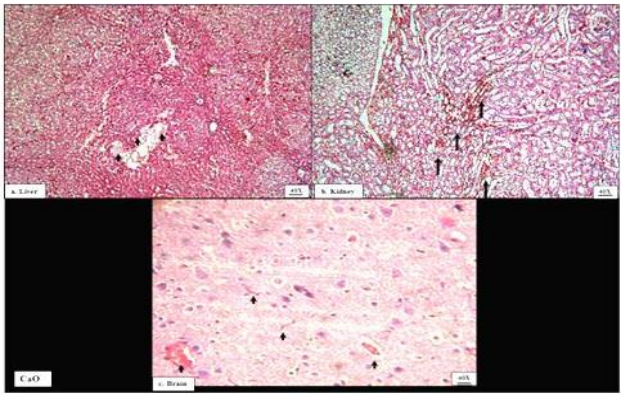

Fig. 4: Harvested sections of liver, kidney and brain after 3 months post-exposure CaO

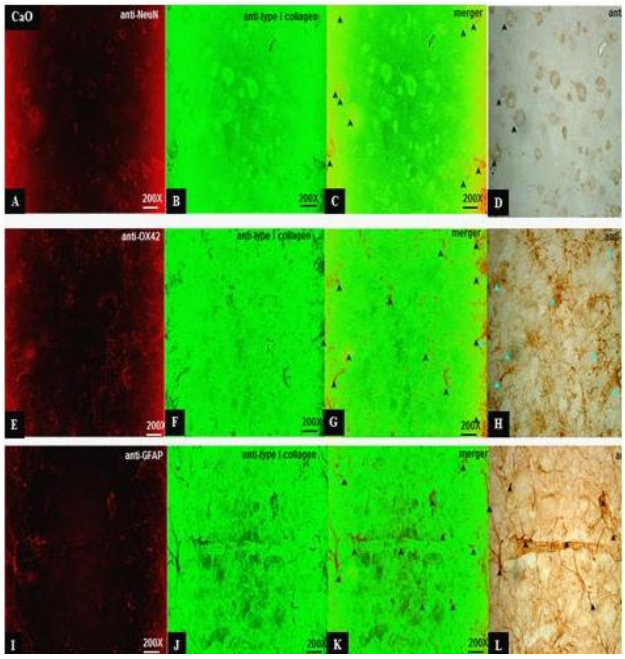

Fig. 5: Conjugation potential of CaO nanowhiskers with neuronal, microglial and astrocytic receptors in rat brain. Anti-type I collagen is used just to determine cellular architecture to get immunofluorescence images

4. Conclusion

Co-precipitation technique was adopted to prepare CaO nanostructure and they were functionalized in PVA. XRD revealed the crystalline nature of CaO and the crystallite size was found to be 4 –11 nm. DSC/TGA and EDS results are in agreement with XRD. SEM result reveals the agglomerated infrastructure of CaO nanowhiskers. The acute toxicity of CaO was investigated in kidney, lungs and brain in rats through H&E staining

protocols. It was observed that introducing CaO resulted in sub-acute hepatic and degenerations were observed in liver and kidney respectively. The mild hemorrhages proved the nanowhiskers crossing blood brain barrier. It was found that CaO bonding with antibodies not detected in immune-fluorescence image. It is suggested that CaO nanomaterial cannot be used directly with antibodies; they need to be modified with appropriate hydrophilic coating. However, these assessments require further studies.

Acknowledgment

The author would like to acknowledge Higher Education Commission, Pakistan for financial support through IRSIP at Cambridge University UK and "Indigenous Ph. D Fellowship Program (5000 Fellowships)". Special thanks to Dr. Munir Ahmad (Nuclear Specialist, Institute of Nuclear Medicine and Oncology Lahore INMOL, Lahore, Pakistan) and Dr. Tousif Hussain (Assistant Prof., Center for Advanced Studies in Physics (CASP), Government College University, Lahore, Pakistan) for guidance in this research.

References

[1] S. Santra and D. Dutta, "Nanoparticles for optical imaging of Cancer", Nanotechnology for life sciences, Editedby Challa Kumar, vol. 7, pp. 48-49, 2007.

[2] P. Li, C. Nan, Z. Wei, J. Lu, Q. Peng and Y. Li, "Mn_3O_4 nanocrystals: facile synthesis, controlled assembly, and application", Chem. Mater., vol. 22, pp. 4232-4236, July 2010.

[3] F. Tian, A.P. Mello, G. Estrada, A. Beyerle, W. Moller, H. Schulz, W. Kreyling and T. Stoeger, "A novel assay for the quantification of internalized nanoparticles in macrophages", Nanotoxicology, vol. 2, pp. 232-242, 2008.

[4] R. L. Edelstein, C. R. Tamanaha, P. E. Sheehan, M. M. Mikker, D. R. Baselt, l. J. Whitman and R. J. Colton, "The BARC biosensor applied to the detection of biological warfare agents", Biosens. Bioelectron., vol. 14, pp. 805-813, January 2000.

[5] J.M. Nam, C.S. Thaxton and C.A. Mirkin, "Nanoparticle-based bio-bar codes for the ultrasensitive detection of proteins", Science, vol. 301, pp. 1884-1886, 2003.

[6] D. Cui, F. Tian, Y. Kong, C. Ozkan, I. Titushikin and H. Gao, "Effects of single-walled carbon nanotubes on the polymerase chain reaction", Nanotechnology, vol. 15, pp. 154-157, 2004.

[7] R.S. Molday and D. Mackenzie, "Immunospecific ferromagnetic iron-dextran reagents for the labeling and magnetic separation of cells", J. Immunol. Methods, vol. 52, pp. 353-367, August 1982.

[8] R. Weissleder, G. Elizondo, J. Wittenberg, C.A. Rabito, H.H. Bengele and L. Josephson, "Ultra small superparamagnetic iron oxide: characterization of a new class of contrast agents for MR imaging", Radiology, vol. 175, pp. 489-493, 1990.

[9] A.C. Eifler and C.S. Thaxton, "Nanoparticle therapeutics: FDA approval, clinical trials, regulatory pathways, and case study" Meth. Mol. Biol., vol. 726, pp. 325-338, January 2011.

[10] Z. Cheng, A. Al-Zaki, J.Z. Hui, V.R. Muzykantov and A. Tsourkas, "Multifunctional nanoparticles: Cost versus benefits of adding targeting and imaging capabilities", Science, vol. 338, pp. 903-910, November 2012.

[11] V. Biju, "Chemical modifications and bioconjugate reactions of nanomaterials for sensing, imaging, drug delivery and therapy" Chem. Soc. Rev., vol. 43, pp. 744-764, February 2014.

[12] E. Neuwelt, N. J. Abbott, L. Abrey, W. A. Banks, B. Blakley, T. Davis, B. Engelhardt, P. Grammas, M. Nedergaard, J. Nutt, W. Pardrige, G.A. Rosenberg, Q. Smith and L.R. Drewes, "Strategies to advance translational research into brain barriers", Lancet Neurol., vol. 7, pp. 84-96, January 2008.

[13] W.M. Pardridge, "Why is the global CNS pharmaceutical market so underpenetrated ?", Drug Discov. Today, vol. 7, pp. 5-7, 2002.

[14] M.W. Bradbury, D.J. Begley and J. Kreuter, "The Blood-brain barrier and drug delivery to the CNS, 1st Edition, Marcel Dekker Inc. USA., 2000.

[15] S. Bhaskar, F. Tian, T. Stoeger, W. Kreyling, J.M. de la Fuente, V. Grazu, P. Borm, G. Estrada, V. Ntziachristos and D. Razansky, "Multifunctional nanocarriers for diagnostics, drug delivery and targeted treatment across blood-brain barrier: Perspectives on tracking and neuroimaging", Part. Fibre Toxicol., vol. 7, pp. 25 pages, 2010.

[16] H.C. Huang, S. Barua, G. Sharma, S.K. Dey and K. Rege, "Inorganic nanoparticles for cancer imaging and therapy", J. Control. Release, vol. 155, pp. 344-357, 2011.

[17] J. Safari and Z. Zarnegar, "Advanced drug delivery systems: Nanotechnology of health design A review", J. Saudi Chem. Soc., vol. 18, pp. 85-89, April 2014.

[18] W. Feng, L.D. Sun, Y.W. Zhang and C.H. Yan, "Synthesis and assembly of rare earth nanostructures directed by the principle of coordination chemistry in solution-based process", Coord. Chem. Rev., vol. 254, pp. 1038-1053, May 2010.

[19] L. Qi, "Colloidal chemical approaches to inorganic micro- and nanostructures with controlled morphologies and patterns", Coordination Chemistry Reviews, vol. 254, pp. 1054-1071, 2010.

[20] D. B. Kuang, A. W. Xu, Y. P. Fang, H. Q. Liu, C. Frommen and D. Fenske, "Surfactant-Assisted Growth of Novel PbS Dendritic Nanostructures via Facile Hydrothermal Process", Adv. Mater., vol. 15, pp. 1747-1750, 2003.

[21] F. Kim, S. Connor, H. Song, T. Kuykendall and P. Yang, "Platonic Gold Nanocrystals", Angew.Chem. Int. Edit., vol. 43, pp. 3673-3677, 2004.

[22] P. N. Nirmala and G. Suresh, "Influence of the particle size on the optical properties of CaO thin film", Inter. J. Recent Scient. Res., vol. 4, pp. 1320-1322, 2013.

[23] M.R. Leonardo, M.E.F.T. Hernandez, L.A. B. Silva and M.T. Filho, "Effect of a calcium hydroxide-based root canal dressing on periapical repair in dogs: a histological study", Oral Radiology and Endodontology, vol. 102, pp. 680-685, November 2006.

[24] Z. Mohammadi and P.M.H. Dummer, "Properties and applications of calcium hydroxide in endodontics and dental traumatology", Int. Endod. J., vol. 44, pp. 697-730, August 2011.

[25] G. Hasselgren, B. Olsson and M. Cvek, "Effects of calcium hydroxide and sodium hypochlorite on the dissolution of necrotic porcine muscle tissue", J. Endod., vol. 14, pp. 125-127, 1988.

[26] K.E. Safavi and F.C. Nichols, "Effect of calcium hydroxide on bacterial lipopolysaccharide", J. Endod., vol. 19, pp. 76-78, February 1993.

[27] J.M. Tanomaru, M.R. Leonardo, T.M. Filho, I.B. Filho and L.A. Silva, "Effect of different irrigation solutions and calcium hydroxide on bacterial LPS", Int.. Endod. J., vol. 36, pp. 733-739, November 2003.

[28] S. Ejaz, D. J. Williamson, T. Ahmed, S. Sitnikov, Y. T. Hong, S. J. Sawaik, T.D. Fryer, F.I. Aigbrihio and J.C. Baron, "Characterizing infarction and selective neuronal loss following temporary focal cerebral ischemia in the rat: A multi-modality imaging study", Neurobiol. Dis., vol. 51, pp. 120-132, 2013.

[29] V. Daniele, G. Taglieri and R. Quaresima, "The nanolimes in cultural heritage conservation: characterization and analysis of the carbonatationprocess", J. Cult. Herit., vol. 9, pp. 294-301, 2008.

[30] S. Datta and D. J. W. Grant, "Effect of supersaturation on the crystallization of phenylbutazone polymorphs", Cryst. Res. Technol., vol. 40, pp. 233-242, March 2005.

[31] A. R. Butt, S. Ejaz, J. C. Baron, M. Ikram and S. Ali, "CaO nanoparticles as a potential drug delivery agent forbiomedical applications", Digest J. Nanomater. Biostruct., vol. 10, pp. 799-809, September 2015.

[32] G. Taglieri, C. Mondelli, V. Daniele, E. Pusceddu and G. Scoccia, "Synthesis, Textural and Structural Properties of Calcium Hydroxide Nanoparticles in Hydro-Alcoholic Suspension", Adv. Mater. Phys. Chem., vol. 4, pp. 50-59, 2014.

[33] H. Yang, C. Zhang, X. Shi, H. Hu, X. Du, Y. Fang, Y. Ma, H. Wu and S. Yang, "Water-soluble super paramagneticmanganese ferritenanoparticles for magnetic resonance imaging", Biomaterials, vol. 31, 3667-3673, 2010.

[34] A. M. Buchan, D. Xue and A. Slivka, "A new model of temporary focal neocortical ischemia in the rat", Stroke, vol. 23, pp. 273-279, 1992.

[35] M. Takasawa, J. S. Beech, T.D. Fryer, Y.T. Hong, J.L. Hughes, K. Igase, P.S. Jones, R. Smith, F.I. Aigbirhio, D.K. Menon, J.C. Clark and J.C. Baron, "Imaging of brain hypoxia in permanent and temporary middle cerebral artery occlusion in the rat using 18F-fluoromisonidazole and positron emission tomography: A pilot study", J. Cereb. Blood Flow Metab., vol. 27, pp. 679-689, April 2007.

[36] J.L. Hughes, J.S. Beech, P.S. Jones, D. Wang, D.K. Menon and J.C. Baron, "Mapping selective neuronal loss and microglial activation in the salvaged neocortical penumbra in the rat", NeuroImage, vol. 49, pp. 19-31, January 2010.

[37] B. D. Cullity and S. R. Stock, "Elements of X-ray Diffraction", 3rd Edition. Prentice Hall: New Jersey, 2001.